Solvent-Driven Formation of Worm-Like Micelles Assembled from a CO2-Responsive Triblock Copolymer

ARTICLE *in* LANGMUIR · JULY 2015

Impact Factor: 4.46 · DOI: 10.1021/acs.langmuir.5b00885 · Source: PubMed

4 AUTHORS, INCLUDING:

Hanbin Liu

Queen's University

13 PUBLICATIONS **77** CITATIONS

SEE PROFILE

Hongyao Yin

Chinese Academy of Sciences

14 PUBLICATIONS **58** CITATIONS

SEE PROFILE

Yujun Feng

Sichuan University

116 PUBLICATIONS **1,366** CITATIONS

SEE PROFILE

Langmuir

Article

pubs.acs.org/Langmuir

Solvent-Driven Formation of Worm-Like Micelles Assembled from a CO_2-Responsive Triblock Copolymer

Hanbin Liu,[†,‡] Wei Wang,[†,‡] Hongyao Yin,[†,‡] and Yujun Feng*[,†,§]

[§]Polymer Research Institute, State Key Laboratory of Polymer Materials Engineering, Sichuan University, Chengdu 610065, People's Republic of China

[†]Chengdu Institute of Organic Chemistry, Chinese Academy of Sciences, Chengdu 610041, People's Republic of China

[‡]University of Chinese Academy of Sciences, Beijing 100049, People's Republic of China

ABSTRACT: Polymer worm-like micelles (WLMs) are difficult to target due to the narrow composition window. In this work, we report polymer WLMs self-assembled from a linear ABC triblock copolymer consisting of an intermediate fluorinated block of poly(2,2,3,4,4,4-hexafluorobutyl methacrylate) (F), a hydrophilic segment of poly(ethylene oxide) (O) and a CO_2-responsive flank of poly(2-(diethylamino)ethyl methacrylate) (E). In the mixed solvent of water and ethanol, the polymer aggregates evolve from spheres to short rods, then long cylinders and finally WLMs when the volume ratio of water increases from 0 to 50%. Upon the stimulus of CO_2, the E block is protonated, thus transforms from hydrophobic to hydrophilic. However, the WLMs just partially return back to spheres even the protonation degree of E block is up to 95%. The closely packed arrangement of fluorinated block caused by the increasing interfacial tension of the fluorinated blocks and solvent could account for the formation of WLMs and its shape alternation under CO_2 stimulus.

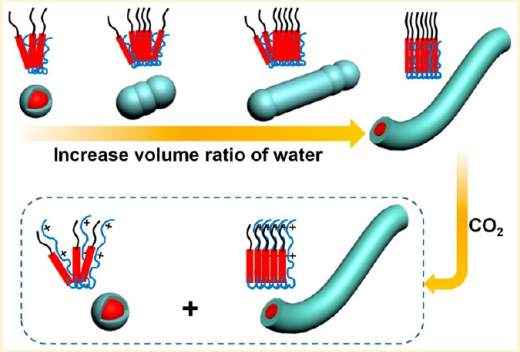

INTRODUCTION

Self-assemblies from block copolymers have attracted considerable attention in recent years because their size, structure, and function can be readily tailored to satisfy specific applications.[1,2] To date, it is well reported that block copolymers in selective solvent can form a variety of self-assemblies with different morphologies including spheres,[3] vesicles,[4,5] cylinders or wormlike micelles (WLMs),[6−8] as well as the exotic multicompartment micelles (MCMs)[9] and Janus micelles.[10,11] Among all of these geometries, WLMs demonstrate some significant advantages over the others in drug delivery, including increased tumor accumulation via enhanced penetration and retention effect, promoted retention time and bioavailability, and improved cellular uptake efficiency.[12,13] Nevertheless, the WLMs are much more difficult to target compared with spheres and vesicles because of their relatively narrow composition window;[14,15] in particular the hydrophilic volume fraction parameter (f_{philic}) is limited within the region between 40% and 50%.[4] An early study[16] based on free energy also proves theoretically a cramped phase region of such cylindrical aggregates.

Despite such a difficulty, some examples of WLMs have been accessed through unremitting efforts. The first approach is precise manipulation of molecular size and composition of block copolymers. Bates' group,[17−20] for instance, discovered a small phase region of WLMs after studying a series of poly(1,2-butadiene)-*b*-poly(ethylene oxide) (PB-*b*-PEO) diblock copolymers with different polymerization degree of PB and weight fraction of PEO. An alternative method for the generation of WLMs is the polymerization-induced self-assembly via living radical polymerization that appeared recently. Typical work is done by Armes and his co-workers[7,8,14,21,22] based on the polymerization of 2-hydroxypropyl methacrylate (HPMA) using a water-soluble macromolecular chain transfer agent. The third strategy should be the introduction of a special segment into block copolymers. For example, Winnik et al.[23−29] fabricated WLMs with diblock copolymers containing polyferrocenylsilane (PFS), which is easy to crystallize in solution, thus producing WLMs. Analogously, O'Reilly and co-workers[15,30] got WLMs with diblock copolymers bearing a crystallizable segment of poly(L-lactide) (PLLA). Besides, using polypeptide as a block, WLMs can be easily developed since the peptide tends to form a one-dimensional β-sheet.[31−33] Similarly, a highly hydrophobic fluorinated polymer may play a role like PFS, PLLA, or peptide in solution. Imae and co-workers[34] discovered ellipsoidal micelles from the fluorinated poly(methacrylic acid)-*b*-poly(perfluorooctylethyl methacrylate) (PMAA-*b*-PFMA) in ethanol solution. Luo et al.[35] found some irregular wormlike structures from fluorinated poly(styrene)-*b*-poly(2,2,3,3,4,4,4-heptafluorobutyl methacrylate) (PS-*b*-PHFBMA) in ethyl acetate. Lodge and coauthors[36] also found wormlike structures

Received: March 9, 2015
Revised: June 25, 2015
Published: July 20, 2015

DOI: 10.1021/acs.langmuir.5b00885
Langmuir 2015, 31, 8756−8763

among the aggregates self-assembled from a miktoarm polymer and believed it is caused by a super strong segregation regime (SSSR) of hydro- and fluorocarbons. However, fine WLMs from the fluorinated linear ABC triblock copolymers have not been achieved yet, so their formation mechanism has not been clarified either. Thus, a new method to develop fine WLMs with a visible process is highly desirable.

Very recently, we fabricated MCMs in pure water in the presence of CO_2 from a linear ABC triblock copolymer, $O_{113}F_{110}E_{212}$, composed of a hydrophilic poly(ethylene oxide) (O), a CO_2-responsive segment poly(2-(diethylamino)ethyl methacrylate) (E), and an intermediate fluorinated block poly(2,2,3,4,4,4-hexafluorobutyl methacrylate) (F) (Scheme 1a).[37] Lodge and co-worker experimentally demonstrated a star polymer containing a fluorinated segment can target a superstrong segregation regime (SSSR).[36] In such an SSSR, the aggregates can only grow in one or two dimensions, which may appear as cylinders or disks.[38] Therefore, the triblock copolymer $O_{113}F_{110}E_{212}$ here is also expected to target SSSR, showing as cylindrical or disk-like microstructure, since it contains a fluorinated in-between block F. However, the SSSR was not successfully achieved in pure water in our previous work.[37] Thus, we wonder if we can fulfill this aim by tuning the environment condition (see solvent) where the triblock copolymer is resided.

Scheme 1. (a) Molecular Structure of Triblock Copolymer $O_{113}F_{110}E_{212}$ and Its Protonation under Stimulation of CO_2; (b) Schematic Representation of the Solvent-Driven Formation of WLMs and Their Morphological Alternation after Exposure of CO_2[a]

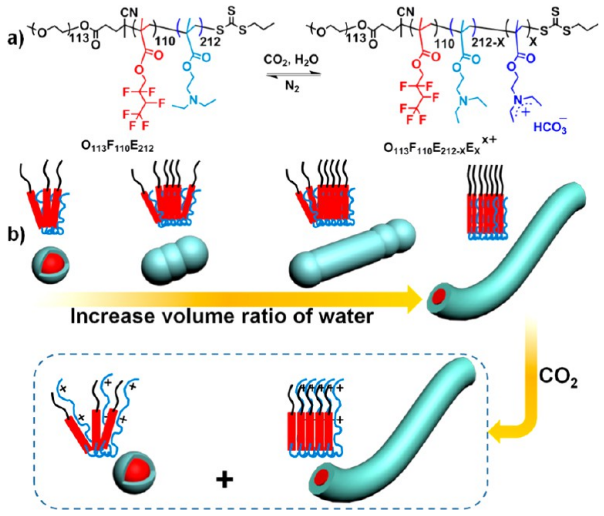

[a]Black wire, O block; red bar, F block; blue fiber. E block.

From the literature,[38] we know that the free energy (F_{free}) of a micelle can be expressed as

$$F_{free} = F_{intf} + F_{core} + F_{corona} \quad (1)$$

where F_{intf}, F_{core}, and F_{corona} are free energies of the interface (including the interaction between polymer and solvent), core, and corona, respectively. By computing these energies, one can get the following relationship[38]

$$R \propto \gamma^{1/3} \quad (2)$$

where R is the radius of the core and γ is the interfacial tension. Such a correlation indicates the size of a micelle is dependent on the interfacial tension in a certain polymer solution. In SSSR, the interfacial energy overwhelms the coronal crowding in solution and R is usually very large, so a higher γ may be the key to target the SSSR.

With this idea in mind, we prepared the assemblies from the triblock copolymer in a mixture of ethanol and water because γ can be enhanced by increasing the volume ratio of water in the mixture solvent. The SSSR is finally achieved, demonstrated as polymer WLMs (a longer cylindrical structure). The shape evolution of the assemblies from spheres to short rods, cylinders, and WLMs is visualized as well. In addition, the E block is sensitive to CO_2, so we wonder if the WLMs can be reversed by CO_2 stimulation, considering the WLMs assembled from a small molecular surfactant could be switched by CO_2.[39] To the best of our knowledge, this is the first example of solvent-driven formation of polymer-based WLMs. Such a process not only may help us understand the formation mechanism of WLMs but also provides a novel strategy for the fabrication of "smart" polymer WLMs.

EXPERIMENTAL SECTION

Materials. The synthesis and characterization of the linear ABC triblock copolymer $O_{113}F_{110}E_{212}$ used in this work were reported in detail previously,[37] and the reference analogue triblock copolymers $O_{113}F_{110}E_{192}$ and $O_{113}F_{110}E_{281}$ were prepared and characterized with the same procedure. The number-average molecular weight (M_n) of the three triblock copolymers is 72, 68, and 84 kDa, respectively, all of which have a PDI around of 1.61. The M_n of the precursor $O_{113}F_{110}$ is 33 kDa with a PDI of 1.35.[37] Ethanol of A.R. grade was purchased from Guanghua Sci-Tech Co., Ltd. (Guangdong, China) and used without further treatment. The deionized water (conductivity κ = 7.9 $\mu S \cdot cm^{-1}$) used in the dialysis process was treated with an ultrapure water purification system (CDUPT-III type, Chengdu Ultrapure Technology Co., Ltd., China). The CO_2 and N_2 gas with a purity of above 99.99% were provided by the Jinnengda Gas Co. in Chengdu, China.

Preparation of Micellar Solutions. Typical procedure for micellar preparation is as follows: 10 mg of copolymer was added into a vial, followed by adding 10 mL of mixture of water and ethanol with a certain volume ratio (from 0 to 80%). After bubbling Ar gas for 15 min, the vials were tightly sealed and stored in an oven at 75 °C for 7 days. The copolymers are gradually dissolved and produce transparent solutions. Thus, the micellar solutions were obtained with a concentration of 1.0 $g \cdot L^{-1}$ after cooling to room temperature. The sample solutions for characterization were equilibrated at least overnight, especially for the solution after CO_2 treatment.

Characterization. *Transmission Electron Microscopy (TEM).* TEM observation was conducted on a Hitachi H600 electron microscope operated at an acceleration voltage of 75 kV. The specimens were prepared by placing about 10 μL of micellar solution on a copper grid coated with carbon film and then stained with 0.2 wt % phosphotungstic acid aqueous solution for 20−30 s, followed by drying in air.

Cryogenic Transmission Electron Microscopy (Cryo-TEM). Cryo-TEM observation and specimen preparation were depicted as follows: About 4 μL of micellar solution was dropped onto a copper grid in a highly humid environment (>90%). Excess solution was soaked by blotting papers, leaving a thin film sprawling on the grid. Then the grid was plunged into liquid ethane, which was frozen by liquid nitrogen. The vitrified samples were transferred into a sample holder (Gatan 626) and observed on a JEOL JEM-1400 TEM (120 kV) at about −174 °C. The images were recorded on a Gatan multiscan CCD camera.

Atomic Force Microscopy (AFM). AFM images were taken in tapping mode with an MFP-3D-BIO atomic force microscope (Asylum

DOI: 10.1021/acs.langmuir.5b00885
Langmuir 2015, 31, 8756−8763

Research, USA) under ambient conditions in air. The diameter of the assemblies was generated from sectional analysis with the software Igor Pro 6.04. To prepare the specimens, a drop of the micellar solution was put on a freshly cleaved mica substrate, followed by lyophilization.

Fluorescence Microscopy (FM). FM images were recorded with a Leica TCS SP8 (Leica, Germany) confocal laser scanning microscope at 570−620 nm (excitation at 552 nm) with an HCX PL APO 63 × 1.4 oil immersion objective. The samples were prepared as follows: 500 μL of micellar solution was taken in an Eppendorf tube, then 10 μL of 0.02 mM fluorescent dye (PKH26, Sigma) was added, and the mixture was then gently mixed. A 10 μL amount of this mixture solution was placed on a glass slide, drying in a vacuum oven, and then washing with deionized water.

Dynamic Light Scattering (DLS). DLS measurement was performed on a Malvern Zetasizer Nano-ZS90 apparatus equipped with a He−Ne laser operated at 633 nm at 25 °C. The scattering angle was fixed at 90° during experiments.

Conductivity and pH Measurements. The conductivity of the micellar solution was determined by an FE30 conductometer (Mettler Toledo, USA) at room temperature. The pH variation was monitored by a Sartorius basic pH meter PB-10 (±0.01) calibrated with standard buffer solutions. The pK_a of the copolymers in aqueous solution was measured following a previously reported procedure.[37] Typically, 5 mL of polymer solution was titrated with 0.002 M hydrochloric acid calibrated by NaOH, while the pH was continuously monitored with the pH meter. The pH corresponding to one-half of the equivalence was taken as the pK_a value.

RESULTS AND DISCUSSION

Solvent-Driven Formation of WLMs. Although it was reported that the fluorinated block copolymers can aggregate into ellipsoidal micelles in ethanol,[30] the fluorinated triblock copolymer $O_{113}F_{110}E_{212}$ used in this work could not directly dissolve in ethanol at room temperature. Thus, we deoxygenized the mixture of the triblock copolymer and solvent (different volume ratio of water in ethanol), sealed the vials (Figure 1), and stored them in the oven at 75 °C for 1 week.

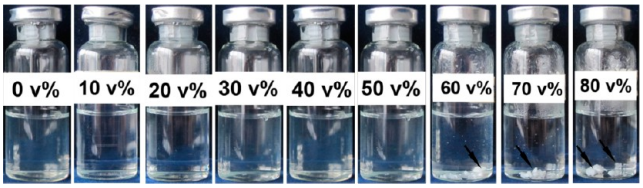

Figure 1. Snapshots of micellar solutions of the triblock copolymer $O_{113}F_{110}E_{212}$ in ethanol/water mixed solution after being stored at 75 °C for 7 days (text in the picture marks the volume ratio of water, and arrows indicate the undissolved polymers after heating).

This storage temperature is higher than the glass transition temperature (T_g) of all segments in the triblock copolymer to guarantee free movement of the polymer chain ($T_{g,O}$ = −70 °C, $T_{g,E}$ = 30−45 °C, $T_{g,F}$ = 68 °C[37]), but lower than the boiling point of ethanol to avoid experimental risk.

After cooling the micellar solution in atmosphere, the sample with a water volume ratio from 0 (pure ethanol) to 50% appears as a colorless and transparent liquid. However, in samples with a water volume ratio higher than 50%, the polymers stay at the bottom of the vials as a precipitant (indicated by arrows in Figure 1).

To figure out the microstructure of polymer aggregates in mixed solvent, TEM was first employed to observe the specimen stained with 0.2 wt % phosphotungstic acid aqueous solution. In pure ethanol solution, only irregular spheres are evidenced (Figure 2a), but an interesting morphological

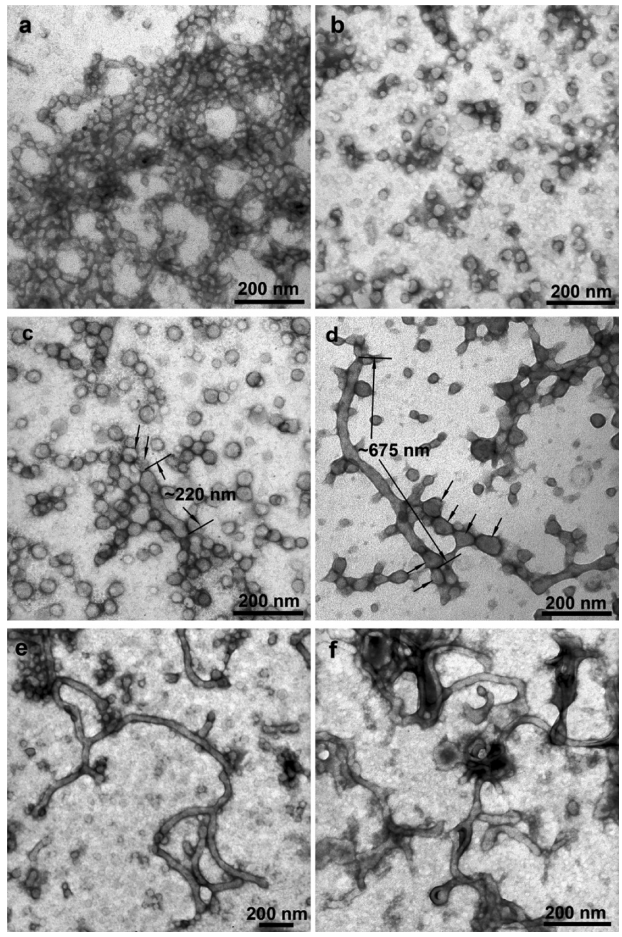

Figure 2. TEM images of self-assemblies from the triblock copolymer $O_{113}F_{110}E_{212}$ in ethanol/water mixture as a function of water volume ratio increasing gradually from a to f: 0, 10%, 20%, 30%, 40%, and 50% (stained with 0.2 wt % phosphotungstic acid). Polymer concentration is 1.0 g·L^{-1}. Bars: 200 nm.

transformation is witnessed when gradually increasing the volume ratio of water, which is a selective solvent for F and E blocks. As exhibited in Figure 2b, uniform spherical micelles with an average diameter of D_{TEM} = 33 nm are observed at 10% water. When the water content reaches 20%, some short rods with a maximum contour length of about L_{TEM} = 220 nm appear (Figure 2c). Remarkably, some spheres tend to aggregate into the rod at the end (see the arrows in Figure 2c), implying the rod grows from spheres. When the water ratio increases to 30%, long cylinders with a contour length of about L_{TEM} = 675 nm show in the TEM photograph (Figure 2d). The growth trace of the cylinder is exposed more significantly than the rods: much more spheres tend to aggregate into the cylinder, although they still retain the appearance of the spherical shapes (indicated by the arrows in Figure 2d). Subsequently, WLMs arise with a length of L_{TEM} = 1−2 μm when the water is continuously added up to 40%. The WLMs contain some branches (Figure 2e), but its diameter still stays at about D_{TEM} = 38 nm, close to the sphere ones in 10% water solution, suggesting the WLMs only grow along the unique one-dimensional (1D) array. It should be pointed out that some spherical micelles still remain as individual particles in such a mixture solution. Nevertheless, the spheres cannot be found when the volume ratio of water is up to 50% (Figure 2f); instead, plenty of WLMs entangle with each other, producing a

DOI: 10.1021/acs.langmuir.5b00885
Langmuir 2015, 31, 8756−8763

network. Interestingly, some structures like vesicles can be found in the image of Figure 2f, implying the WLMs may tend to transform into other shapes. Unfortunately, when the volume ratio of water is larger than 50%, the triblock copolymer would precipitate at the bottom of the vials (Figure 1, indicated by the arrows); thus, no assemblies can be achieved in a higher content of water based on the present self-assembly method. In short, a full scenario of transformation from spheres to short rods, then to long cylinders, and finally to WLMs is obtained from the TEM visualization with a staining technique of phosphotungstic acid.

To corroborate the morphological transformation and exclude the possible artifacts from staining during TEM specimen preparation, cryo-TEM was further employed to observe the aggregates free of staining. As shown in Figure 3a

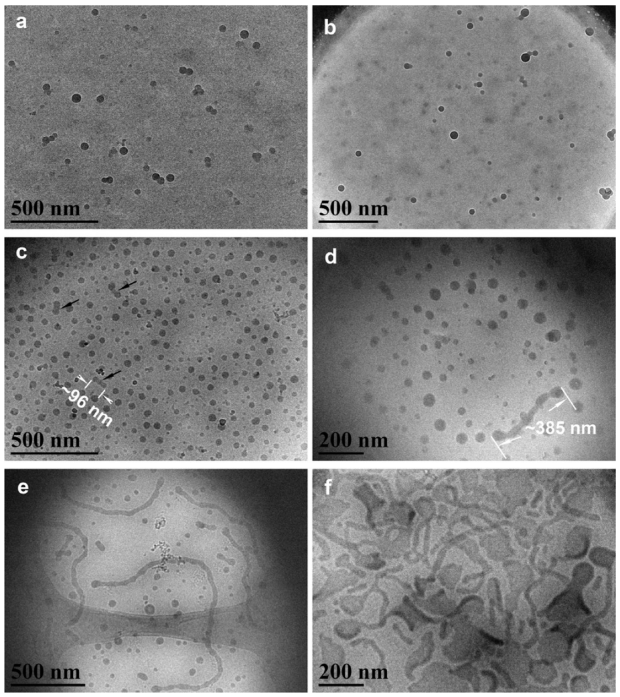

Figure 3. Cryo-TEM images of self-assemblies (without staining) from the triblock copolymer $O_{113}F_{110}E_{212}$ in ethanol/water mixture as the volume ratio of water increasing gradually from a to f: 0, 10%, 20%, 30%, 40%, and 50%. Polymer concentration is fixed at 1.0 g·L^{-1}. Bars for a, b, c, and e: 500 nm. Bars for d and f: 200 nm.

and 3b, when the volume ratio of water is lower than 20%, only spheres can be visualized with an average diameter of $D_{\text{cryo-TEM}}$ = 45 nm. This size agrees well with the TEM result (D_{TEM} = 33 nm Figure 2b) considering the drying operation in the TEM technique. When the water content increases to 20%, some short rods can be found (Figure 3c, indicated by the arrows). One of such rods has a contour length of about 96 nm and a diameter of around 30 nm, implying it is stacked by two or three spheres. When the water loading is up to 30%, a long cylinder with a contour length of above 385 nm is observed (Figure 3d). Noticeably, the long cylinder still keeps some significant trace of sphere which looks like a string of beads, indicating it grows from spheres. This discovery is consistent with the TEM findings (Figure 2c and 2d). When the volume ratio of water increases to 40%, WLMs appear accompanied by some spheres (Figure 3e). Finally, the WLMs aggregate into a network when the water content is raised up to 50% (Figure 3f), in good accordance with TEM observation (Figure 2f). Besides, the appearance of a vesicles-like structure looks more obvious compared with that in the TEM image (Figure 2f), indicating a possible transition from WLMs to vesicles. The cryo-TEM observation further supports the TEM results, demonstrating the aggregates evolve from spherical micelles to short rods, then to long cylinders, and finally to WLMs when the volume ratio of water increases gradually. This accordance also indicates that the staining operation has no impact on the observation of WLMs; thus, the TEM technique can be used in the following visualization of WLMs.

Except for the TEM and cryo-TEM observation, the WLMs formed in mixed solvent with a water ratio of 50% were also visualized by FM and AFM. The fiber-like structure in Figure 4a

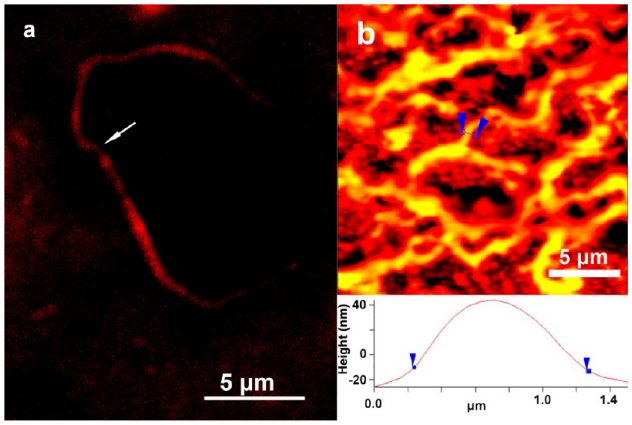

Figure 4. (a) Fluorescence microscopy images and (b) AFM photograph of WLMs assembled from the triblock copolymer $O_{113}F_{110}E_{212}$ in ethanol/water mixture with water ratio of 50%. Polymer concentration is 1.0 g·L^{-1}.

is a typical image of WLMs in the sight of FM. The fluorescence dye PKH26 was loaded into the WLMs by direct addition into the polymer solution; thus, the red ribbon should be ascribed to the WLMs. Its contour length is around 20 μm, which is larger than that observed by TEM and cryo-TEM because it is composed of two WLMs with a junction (see arrow in Figure 4a) in the middle. The diameter in this picture shows about 550 nm, much larger than those observed from TEM (38 nm) and cryo-TEM (45 nm), because the resolution limit of FM cannot reach those of the TEM instruments. In the AFM image of Figure 4b, networks of WLMs can be clearly distinguished. The cross-sectional analysis shows a single peak with a height of about 50 nm, comparable with the diameter of D_{TEM} (38 nm) and $D_{\text{cryo-TEM}}$ (45 nm) (Figures 2 and 3). However, the distance from the baseline (indicated by blue arrows in Figure 4b) is over 1 μm, suggesting about 20 WLMs rather than 1 single WLM parallelly align in this region.

After visualizing the morphological evolution of the WLMs, the hydrodynamic diameter (D_h) of the aggregate with different water content was studied by DLS. As shown in Figure 5, D_h gradually extends with the volume ratio of water increasing in the mixture, agreeing with the morphological transformation from spheres to a short rod, then to a long cylinder, and finally to WLMs. In pure ethanol, D_h is only 10 nm, but it turns to 58 nm when the water content increases to 10%, in line with the TEM and cryo-TEM observations (D_{TEM} = 33 nm and $D_{\text{cryo-TEM}}$ = 45 nm). When the volume ratio of water increases to 20%, D_h rises to 142 nm, comparable with the length of short

DOI: 10.1021/acs.langmuir.5b00885
Langmuir 2015, 31, 8756−8763

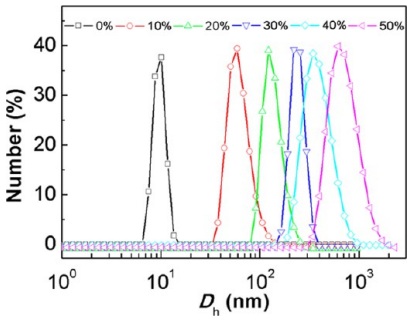

Figure 5. DLS data of aggregates from the triblock copolymer $O_{113}F_{110}E_{212}$ in ethanol/water mixture with different volume ratios of water. Polymer concentration is fixed at 1.0 g·L^{-1}.

cylinders observed by TEM (~220 nm) and cryo-TEM (~96 nm). Finally, the D_h gets up to 615 nm when the water content is raised to 50%, indicating the spherical micelles are transformed into WLMs. The difference between this datum with the counter length observed by TEM, cryo-TEM, or FM is caused by the calculation method of D_h based on spheres instead of fiber-like structure.

Influence of Polymer Concentration on the Formation of WLMs. Apart from solvent composition, it is well recognized that polymer concentration may also influence the morphology of polymer self-assemblies.[2] Thus, the concentration dependence of aggregates was examined at a constant water content of 50% in the mixture. As shown in Figure 6a and 6b, when

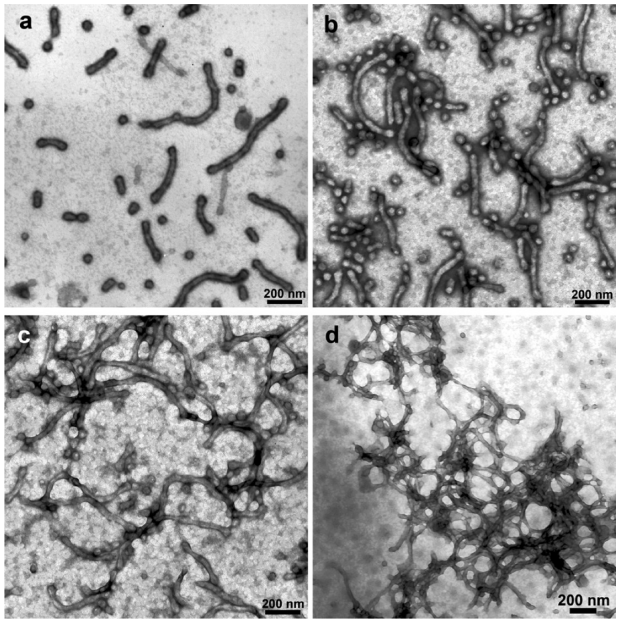

Figure 6. TEM images of the self-assemblies from the triblock copolymer $O_{113}F_{110}E_{212}$ with different polymer concentrations in the mixture of ethanol/water at a fixed water content of 50% stained with 0.2 wt % phosphotungstic acid. (a, b, c, and d) Polymer concentration is 0.2, 0.5, 2.0, and 5.0 g·L^{-1}, respectively. Bars: 200 nm.

polymer concentration is lower than 1.0 g·L^{-1} (0.2 and 0.5 g·L^{-1}, respectively), rods and cylinders with a length of about 100−400 nm dominate the system, accompanying some spherical micelles. When the polymer concentration increases to 2.0 g·L^{-1}, WLMs are formed (Figure 6c), which are identical with the aggregates at 1.0 g·L^{-1} (Figures 2f and 3f). When the polymer concentration further rises up to 5.0 g·L^{-1}, the formed WLMs entangled with each other to yield an intensive network (Figure 6d). These morphological changes indicate the formation of WLMs has a positive correlation with the polymer concentration in the mixed solvent, because the growth of micelles is dynamically limited from spheres to WLMs in low polymer concentration (see Figure 1c, 1d, 2c, and 2d). At higher concentration, more spheres form in solution to produce more chances to grow toward WLMs.

Influence of the E Block Length on WLMs. The molecular structure variation of copolymers might be another important influential factor on the morphologies. As exhibited in Figure 7a and 7b, the triblock copolymers $O_{113}F_{110}E_{192}$ and

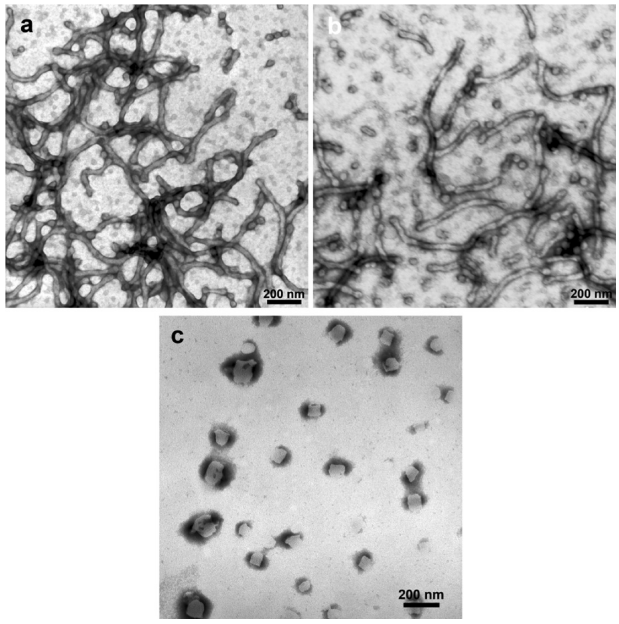

Figure 7. TEM images of self-assemblies for (a) triblock copolymer $O_{113}F_{110}E_{192}$, (b) $O_{113}F_{110}E_{281}$, and (c) diblock precursor $O_{113}F_{110}$ in ethanol/water mixture with a water content of 50% stained with 0.2 wt % phosphotungstic acid. Polymer concentration is fixed at 1.0 g·L^{-1}. Bars: 200 nm.

$O_{113}F_{110}E_{281}$, analogous to the above-mentioned $O_{113}F_{110}E_{212}$ in structure but differing in E block length, can also aggregate into WLMs in 50% mixed solvent of water and ethanol, implying the formation of WLMs is independent of the block length of E segment. Does this mean the E block is dispensable for the formation of the WLMs? To answer this question, the self-assembly of the diblock precursor $O_{113}F_{110}$ was checked as well. Interestingly, only irregular spherical micelles (Figure 7c) were observed. This suggests that the E block is necessary for the formation of WLMs, since it should benefit the arrangement of the triblock copolymer during their growth from spheres to WLMs.

Phase Diagram of Self-Assemblies from the Triblock Copolymer $O_{113}F_{110}E_{212}$. On the basis of the above findings, a phase diagram of the triblock copolymer $O_{113}F_{110}E_{212}$ in water/ethanol mixed solutions was drawn (Figure 8) to show the evolution of the aggregates upon increasing polymer concentration and water content. At a fixed polymer concentration of 1.0 g·L^{-1}, when increasing the water content from 0 to 50%, spherical micelles are first formed and then grow into short rods, successively cylinders, and finally WLMs (seen along the

DOI: 10.1021/acs.langmuir.5b00885
Langmuir 2015, 31, 8756−8763

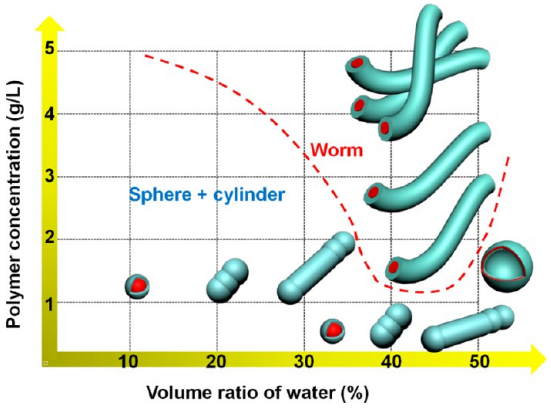

Figure 8. Phase diagram of the triblock copolymer $O_{113}F_{110}E_{212}$ in water/ethanol mixed solvent as a function of volume ratio of water and polymer concentration.

X axis in Figure 8). If the water content is fixed at 50%, a transition from the coexistence of spheres, rods, and cylinders to WLMs, finally entangled WLMs networks are expected upon increasing polymer concentration from 0.2 to 5.0 g·L^{-1} (shown along the *Y* axis in Figure 8). From this 2-D diagram, a semi-U shaped boundary can be highlighted (red dashed curve in Figure 8). Below the curve, the triblock copolymer $O_{113}F_{110}E_{212}$ aggregates into spheres, rods, and cylinders; above the line, the copolymer self-assembles into WLMs. Such a phase diagram may be helpful to guide the design and fabrication of WLMs from fluorinated triblock copolymers in mixed solvent.

Morphological Transition upon CO_2 Stimulus. Although the formation of WLMs by gradually increasing the volume ratio of water is well demonstrated, it is interesting to see if the WLMs can return back to spheres because the E block is a CO_2-sensitive moiety which is widely studied in recent years,[39−47] and we found recently the triblock copolymer $O_{113}F_{110}E_{212}$ can assemble into CO_2-switchable MCMs in pure water.[37] Lots of spherical micelles appear in the mixed solvent after treatment with CO_2 as shown in Figure 9a; however, some WLMs remain in solution, indicating they cannot completely return back to spheres by bubbling CO_2. One reason for this partial transformation may be the shorter equilibration time compared with the WLMs formation process. Usually it takes 1 week to prepare WLMs in our experiment as mentioned above, but we check the morphology on the next day after bubbling CO_2. To clarify this confusion, the micellar solution after CO_2 treatment was left to equilibrate for 7 days at room temperature and then check TEM again. As shown in Figure 9b, some WLMs can be observed as well, indicating the transformation in mixed solvent is difficult to achieve.

Considering the possible impact of ethanol on the CO_2 responsiveness of E block, the WLMs were dialyzed against pure water, keeping the polymer concentration at 1.0 g·L^{-1}. The CO_2 sensitivity was first confirmed by monitoring the pH and conductivity while CO_2 was bubbling into the aqueous micellar solution. As shown in Figure 9c, the conductivity of the micellar solution dramatically increases from 35.2 to 89.2 μS·cm^{-1} in 6 min and finally climbs to 104.0 μS·cm^{-1} after bubbling CO_2 for 20 min, a nearly 3 times increase compared with the initial value. Such a jump in conductivity results from the production of conductive ions in aqueous solution, which should be the bicarbonate produced by the reaction of tertiary amine groups with CO_2.[46,47] Concurrently, the pH decreases from 7.02 to 4.65, demonstrating the protonation of tertiary

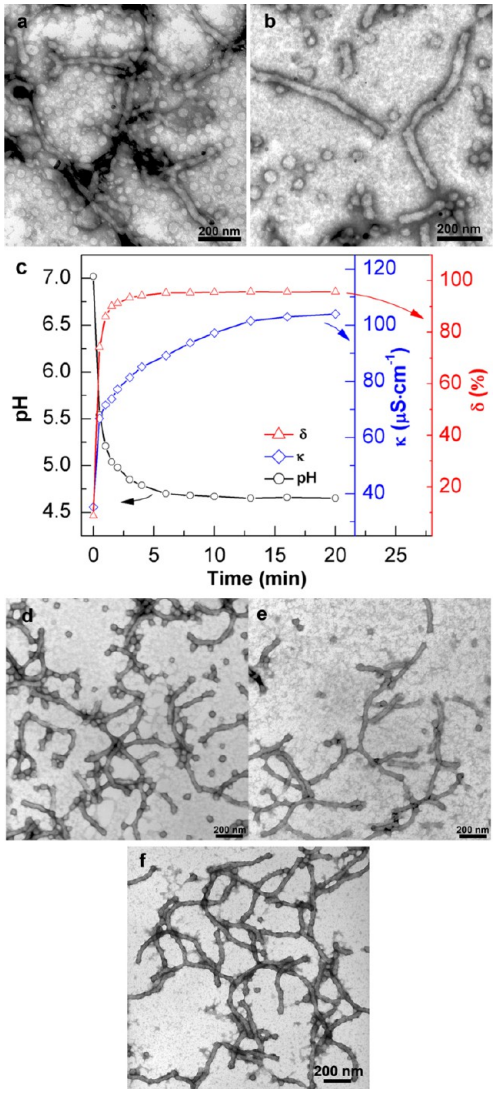

Figure 9. (a and b) TEM image of the self-assemblies from the triblock copolymer $O_{113}F_{110}E_{212}$ in ethanol/water mixture with a water volume ratio of 50% after bubbling CO_2 (a, equilibrate overnight; b, equilibrate for 7 days); (c) pH, conductivity (κ), and protonated degree (δ) of the aqueous micellar solution for $O_{113}F_{110}E_{212}$ as a function of CO_2 bubbling time (15 mL·min^{-1}) in water; (d−f) TEM images of aggregates from $O_{113}F_{110}E_{212}$ after dialysis into pure water (d, before bubbling CO_2; e, after bubbling CO_2; f, after ultrasonic treatment for 30 min without CO_2 treatment). Polymer concentration fixed at 1.0 g·L^{-1}. All specimens for TEM observation are stained with 0.2 wt % phosphotungstic acid.

amine groups in the E block. In order to get the degree of protonation (δ), the pK_a of the polymer $O_{113}F_{110}E_{212}$ was titrated at 6.0 with 0.02 M HCl solution using a previously described procedure.[37] As given in Figure 9c, δ is as low as 8.7% before aeration of CO_2; then it quickly rises to 95% in 6 min upon treatment of CO_2 and finally keeps constant until 20 min of CO_2 bubbling. Remarkably, δ shows the same change pace with that of pH (the significant change occurs in first 6 min), indicating protonation of tertiary amines is the exact reason causing the variation of pH in the micellar solution.

Now that the E block can be protonated (as high as 95%) in aqueous solution, we wonder if the morphological transition occurs correspondingly after the reaction with CO_2. However, as shown in Figure 9d and 9e, the aggregates still appear as

DOI: 10.1021/acs.langmuir.5b00885
Langmuir 2015, 31, 8756−8763

WLMs before and after treatment with CO_2, implying the protonation is insufficient to drive a morphological transition for the WLMs in water. This phenomenon may be related with the special arrangement of F block in the aggregates, so we attempt to break the arrangement of F blocks by ultrasonic treatment. After dialysis of the triblock copolymer $O_{113}F_{110}E_{212}$ against pure water, the micellar solution was treated with an ultrasonic machine for 30 min and then observed with TEM. Nevertheless, as shown in Figure 9f, the formed WLMs remains unchanged, implying the F block is closely packed together in the self-assemblies, so the morphology cannot be reversed by either CO_2 stimulus or strong physical treatment.

Taking all the above results into consideration, a tentative mechanism is proposed to comprehend the formation of WLMs in selective solvent and their partial morphological alternation upon CO_2 stimulus. The interfacial energy between the fluorinated F block and water should be the engine to drive the formation of WLMs. On the basis of what was reported by Imae and co-workers[34] on the assemblies of fluorinated block copolymers, here a model of triblock copolymer is established with a rod-like F segment and two coil-like segments (O and E) (Figure 1b). When water content is less than 20% or in pure ethanol, the interfacial energy (F_{intf}) is quite small due to the low γ between F block and water, producing spherical micelles with a core of hydrophobic E and F blocks and shell of hydrophilic O block. When the water loading increases to 20−30%, γ between F segments and water increases significantly and causes the accumulation of F_{intf}. In this situation, some F units arrange in parallel to balance the increased F_{intf}, resulting in rods and cylinders. When the water content rises up to 40−50%, F_{intf} further increases and targets the so-called SSSR, which induces closely packed arrangement of F blocks to minimize the high F_{intf} by decreasing the interfacial area. As a result, WLMs are eventually targeted.

After bubbling CO_2 into the mixed solvent, a portion of the WLMs converts back into spherical micelles because of the electrostatic repulsion between charged E blocks. However, the reverse is not completely due to the strong interfacial energy between F and water. Then after dialysis into water, the F blocks pack more closely since they are surrounded by more water. The repulsion of charged E blocks (even δ goes up to 95%) cannot push the rearrangement of F blocks, so the WLMs remain unchanged. These stable WLMs in water, from another point, approve the closely packed arrangement of F block granted by the SSSR mechanism, thus supporting the above mechanism. Another obvious proof is that the WLMs cannot be destroyed even upon ultrasonic treatment for 30 min, demonstrating the close arrangement again. In other words, the enhanced interfacial energy during increasing water content produces the WLMs from step-by-step shape evolution, but the SSSR of WLMs makes are hard to reverse.

CONCLUSIONS

Polymer-based WLMs driven by gradient variation of solvent composition has been demonstrated with a linear ABC triblock copolymer. The evolution from spherical micelles to short rods, then cylinders, and finally WLMs is visualized when the water volume ratio gradually increases from 0 to 50% in the mixed solvent of water and ethanol. Furthermore, a higher polymer concentration favors the formation of WLMs, while the length of E block shows less impact. The gradually closer packed arrangement of fluorinated F block driven by accumulated interfacial energy can account for the morphological transformation and makes the WLMs remain stable under CO_2 stimulus even under ultrasonic treatment. This simple solvent-driven method may pave a new way for the fabrication of polymer WLMs. Considering the good biocompatibility and membrane permeability of CO_2, CO_2-triggered drug delivery WLMs are promising to target in the future based on the present method.

AUTHOR INFORMATION

Corresponding Author

*E-mail: yjfeng@scu.edu.cn.

Notes

The authors declare no competing financial interest.

ACKNOWLEDGMENTS

The authors would like to thank the financial support from the National Natural Science Foundation of China (21273223, 21173207), and the Distinguished Youth Fund of Sichuan Province (2010JQ0029).

REFERENCES

(1) Blanazs, A.; Armes, S. P.; Ryan, A. J. Self-assembled block copolymer aggregates: from micelles to vesicles and their biological applications. *Macromol. Rapid Commun.* **2009**, *30*, 267−277.

(2) Mai, Y.; Eisenberg, A. Self-assembly of block copolymers. *Chem. Soc. Rev.* **2012**, *41*, 5969−5985.

(3) Gao, Z.; Varshney, S. K.; Wong, S.; Eisenberg, A. Block copolymer crew-cut micelles in water. *Macromolecules* **1994**, *27*, 7923−7927.

(4) Discher, D. E.; Eisenberg, A. Polymer vesicles. *Science* **2002**, *297*, 967−973.

(5) Du, J.; O'Reilly, R. K. Advances and challenges in smart and functional polymer vesicles. *Soft Matter* **2009**, *5*, 3544−3561.

(6) Fernyhough, C.; Ryan, A. J.; Battaglia, G. pH controlled assembly of a polybutadiene-poly(methacrylic acid) copolymer in water: packing considerations and kinetic limitations. *Soft Matter* **2009**, *5*, 1674−1682.

(7) Warren, N. J.; Mykhaylyk, O. O.; Mahmood, D.; Ryan, A. J.; Armes, S. P. RAFT aqueous dispersion polymerization yields poly(ethylene glycol)-based diblock copolymer nano-objects with predictable single phase morphologies. *J. Am. Chem. Soc.* **2014**, *136*, 1023−1033.

(8) Fielding, L. A.; Lane, J. A.; Derry, M. J.; Mykhaylyk, O. O.; Armes, S. P. Thermo-responsive diblock copolymer worm gels in non-polar solvents. *J. Am. Chem. Soc.* **2014**, *136*, 5790−5798.

(9) Gröschel, A. H.; Schacher, F. H.; Schmalz, H.; Borisov, O. V.; Zhulina, E. B.; Walther, A.; Müller, A. H. E. Precise hierarchical self-assembly of multicompartment micelles. *Nat. Commun.* **2012**, *3*, 710−720.

(10) Gröschel, A. H.; Walther, A.; Lobling, T. I.; Schmelz, J.; Hanisch, A.; Schmalz, H.; Müller, A. H. E. Facile, solution-based synthesis of soft, nanoscale Janus particles with tunable Janus balance. *J. Am. Chem. Soc.* **2012**, *134*, 13850−13860.

(11) Gröschel, A. H.; Lobling, T. I.; Petrov, P. D.; Mullner, M.; Kuttner, C.; Wieberger, F.; Muller, A. H. E. Janus micelles as effective supracolloidal dispersants for carbon nanotubes. *Angew. Chem., Int. Ed.* **2013**, *52*, 3602−3606.

(12) Geng, Y.; Dalhaimer, P.; Cai, S.; Tsai, R.; Tewari, M.; Minko, T.; Discher, D. E. Shape effects of filaments versus spherical particles in flow and drug delivery. *Nat. Nanotechnol.* **2007**, *2*, 249−255.

(13) Yu, H.; Xu, Z.; Wang, D.; Chen, X.; Zhang, Z.; Yin, Q.; Li, Y. Intracellular pH-activated PEG-*b*-PDPA wormlike micelles for hydrophobic drug delivery. *Polym. Chem.* **2013**, *4*, 5052−5055.

(14) Blanazs, A.; Verber, R.; Mykhaylyk, O. O.; Ryan, A. J.; Heath, J. Z.; Douglas, C. I.; Armes, S. P. Sterilizable gels from thermoresponsive block copolymer worms. *J. Am. Chem. Soc.* **2012**, *134*, 9741−9748.

DOI: 10.1021/acs.langmuir.5b00885
Langmuir 2015, 31, 8756−8763

(15) Sun, L.; Petzetakis, N.; Pitto-Barry, A.; Schiller, T. L.; Kirby, N.; Keddie, D. J.; Boyd, B. J.; O'Reilly, R. K.; Dove, A. P. Tuning the size of cylindrical micelles from poly(*L*-lactide)-*b*-poly(acrylic acid) diblock copolymers based on crystallization-driven self-assembly. *Macromolecules* **2013**, *46*, 9074−9082.
(16) Zhulina, E. B.; Adam, M.; LaRue, I.; Sheiko, S. S.; Rubinstein, M. Diblock copolymer micelles in a dilute solution. *Macromolecules* **2005**, *38*, 5330−5351.
(17) Won, Y.-Y.; Davis, H. T.; Bates, F. S. Giant wormlike rubber micelles. *Science* **1999**, *283*, 960−963.
(18) Won, Y.-Y.; Paso, K.; Davis, H. T.; Bates, F. S. Comparison of original and cross-linked wormlike micelles of poly(ethylene oxide-*b*-butadiene) in water: rheological properties and effects of poly(ethylene oxide) addition. *J. Phys. Chem. B* **2001**, *105*, 8302−8311.
(19) Jain, S.; Bates, F. S. On the origins of morphological complexity in block copolymer surfactants. *Science* **2003**, *300*, 460−464.
(20) Jain, S.; Bates, F. S. Consequences of nonergodicity in aqueous binary PEO-PB micellar dispersions. *Macromolecules* **2004**, *37*, 1511−1523.
(21) Blanazs, A.; Madsen, J.; Battaglia, G.; Ryan, A. J.; Armes, S. P. Mechanistic insights for block copolymer morphologies: how do worms form vesicles? *J. Am. Chem. Soc.* **2011**, *133*, 16581−16587.
(22) Sugihara, S.; Blanazs, A.; Armes, S. P.; Ryan, A. J.; Lewis, A. L. Aqueous dispersion polymerization: a new paradigm for in situ block copolymer self-assembly in concentrated solution. *J. Am. Chem. Soc.* **2011**, *133*, 15707−15713.
(23) Massey, J.; Power, K. N.; Manners, I.; Winnik, M. A. Self-assembly of a novel organometallic−inorganic block copolymer in solution and the solid state: nonintrusive observation of novel wormlike poly(ferrocenyldimethylsilane)-*b*-poly(dimethylsiloxane) micelles. *J. Am. Chem. Soc.* **1998**, *120*, 9533−9540.
(24) Massey, J. A.; Temple, K.; Cao, L.; Rharbi, Y.; Raez, J.; Winnik, M. A.; Manners, I. Self-assembly of organometallic block copolymers: the role of crystallinity of the core-forming polyferrocene block in the micellar morphologies formed by poly(ferrocenylsilane-*b*-dimethylsiloxane) in *n*-alkane solvents. *J. Am. Chem. Soc.* **2000**, *122*, 11577−11584.
(25) Wang, X. S.; Arsenault, A.; Ozin, G. A.; Winnik, M. A.; Manners, I. Shell-cross-linked cylindrical polyisoprene-*b*-polyferrocenylsilane (PI-*b*-PFS) block copolymer micelles: one-dimensional (1D) organometallic nanocylinders. *J. Am. Chem. Soc.* **2003**, *125*, 12686−12687.
(26) Wang, X. S.; Winnik, M. A.; Manners, I. Swellable, redox-active shell-crosslinked organometallic nanotubes. *Angew. Chem., Int. Ed.* **2004**, *43*, 3703−3707.
(27) Wang, X. S.; Wang, H.; Coombs, N.; Winnik, M. A.; Manners, I. Redox-induced synthesis and encapsulation of metal nanoparticles in shell-cross-linked organometallic nanotubes. *J. Am. Chem. Soc.* **2005**, *127*, 8924−8925.
(28) Wang, X.; Guerin, G.; Wang, H.; Wang, Y.; Manners, I.; Winnik, M. A. Cylindrical block copolymer micelles and co-micelles of controlled length and architecture. *Science* **2007**, *317*, 644−647.
(29) Gädt, T.; Ieong, N. S.; Cambridge, G.; Winnik, M. A.; Manners, I. Complex and hierarchical micelle architectures from diblock copolymers using living, crystallization-driven polymerizations. *Nat. Mater.* **2009**, *8*, 144−150.
(30) Petzetakis, N.; Dove, A. P.; O'Reilly, R. K. Cylindrical micelles from the living crystallization-driven self-assembly of poly (lactide)-containing block copolymers. *Chem. Sci.* **2011**, *2*, 955−960.
(31) Chen, L.; Chen, T.; Fang, W.; Wen, Y.; Lin, S.; Lin, J.; Cai, C. Synthesis and pH-responsive "schizophrenic" aggregation of a linear-dendron-like polyampholyte based on oppositely charged polypeptides. *Biomacromolecules* **2013**, *14*, 4320−4330.
(32) Shimada, T.; Sakamoto, N.; Motokawa, R.; Koizumi, S.; Tirrell, M. Self-assembly process of peptide amphiphile worm-like micelles. *J. Phys. Chem. B* **2012**, *116*, 240−243.
(33) Xu, H.; Wang, J.; Han, S.; Wang, J.; Yu, D.; Zhang, H.; Xia, D.; Zhao, X.; Waigh, T. A.; Lu, J. R. Hydrophobic-region-induced transitions in self-assembled peptide nanostructures. *Langmuir* **2009**, *25*, 4115−4123.
(34) Ito, H.; Imae, T.; Nakamura, T.; Sugiura, M.; Oshibe, Y. Self-association of water-soluble fluorinated diblock copolymers in solutions. *J. Colloid Interface Sci.* **2004**, *276*, 290−298.
(35) Zhou, Y. N.; Cheng, H.; Luo, Z. H. Fluorinated AB diblock copolymers and their aggregates in organic solvents. *J. Polym. Sci., Part A: Polym. Chem.* **2011**, *49*, 3647−3657.
(36) Li, Z. B.; Kesselman, E.; Talmon, Y.; Hillmyer, M. A.; Lodge, T. P. Multicompartment micelles from ABC miktoarm stars in water. *Science* **2004**, *306*, 98−101.
(37) Liu, H.; Zhao, Y.; Dreiss, C. A.; Feng, Y. CO_2-switchable multicompartment micelles with segregated corona. *Soft Matter* **2014**, *10*, 6387−6391.
(38) Semenow, A. N.; Nyrkova, I. A.; Khokhlov, A. R. Polymers with strongly interacting groups: theory for nonspherical multiplets. *Macromolecules* **1995**, *28*, 7491−7500.
(39) Su, X.; Cunningham, M. F.; Jessop, P. G. Switchable viscosity triggered by CO_2 using smart worm-like micelles. *Chem. Commun.* **2013**, *49*, 2655−2657.
(40) Han, D.; Tong, X.; Boissière, O.; Zhao, Y. General strategy for making CO_2-switchable polymers. *ACS Macro Lett.* **2012**, *1*, 57−61.
(41) Zhang, J. M.; Han, D. H.; Zhang, H. J.; Chaker, M.; Zhao, Y.; Ma, D. L. In situ recyclable gold nanoparticles using CO_2-switchable polymers for catalytic reduction of 4-nitrophenol. *Chem. Commun.* **2012**, *48*, 11510−11512.
(42) Kumar, S.; Tong, X.; Dory, Y. L.; Lepage, M.; Zhao, Y. A CO_2-switchable polymer brush for reversible capture and release of proteins. *Chem. Commun.* **2013**, *49*, 90−92.
(43) Yan, B.; Han, D. H.; Boissiere, O.; Ayotte, P.; Zhao, Y. Manipulation of block copolymer vesicles using CO_2: dissociation or "breathing". *Soft Matter* **2013**, *9*, 2011−2016.
(44) Yan, Q.; Zhao, Y. CO_2-stimulated diversiform deformations of polymer assemblies. *Angew. Chem., Int. Ed.* **2013**, *52*, 9948−51.
(45) Yan, Q.; Zhao, Y. CO_2-stimulated diversiform deformations of polymer assemblies. *J. Am. Chem. Soc.* **2013**, *135*, 16300−16303.
(46) Liu, H.; Guo, Z.; He, S.; Yin, H.; Fei, C.; Feng, Y. CO_2-driven vesicle to micelle regulation of amphiphilic copolymer: random versus block strategy. *Polym. Chem.* **2014**, *5*, 4756−4763.
(47) Zhang, Y.; Chu, Z.; Dreiss, C. A.; Wang, Y.; Fei, C.; Feng, Y. Smart wormlike micelles switched by CO_2 and air. *Soft Matter* **2013**, *9*, 6217−6221.
(48) Zhang, Y.; Feng, Y.; Wang, J.; He, S.; Guo, Z.; Chu, Z.; Dreiss, C. A. CO_2-switchable wormlike micelles. *Chem. Commun.* **2013**, *49*, 4902−4904.

DOI: 10.1021/acs.langmuir.5b00885
Langmuir 2015, 31, 8756−8763